Quantitative Flood Forecasting Using Remotely-Sensed Data and Neural Networks

Kim, Gwangseob
Department of Civil Engineering, Kyungpook National University, Daegu, Korea

ABSTRACT: Accurate quantitative forecasting of rainfall for basins with a short response time is essential to predict streamflow and flash floods. Previously, neural networks were used to develop a Quantitative Precipitation Forecasting (QPF) model that highly improved forecasting skill at specific locations in Pennsylvania, using both Numerical Weather Prediction (NWP) output and rainfall and radiosonde data. The objective of this study was to improve an existing artificial neural network model and incorporate the evolving structure and frequency of intense weather systems in the mid-Atlantic region of the United States for improved flood forecasting. Besides using radiosonde and rainfall data, the model also used the satellite-derived characteristics of storm systems such as tropical cyclones, mesoscale convective complex systems and convective cloud clusters as input. The convective classification and tracking system (CCATS) was used to identify and quantify storm properties such as life time, area, eccentricity, and track. As in standard expert prediction systems, the fundamental structure of the neural network model was learned from the hydroclimatology of the relationships between weather system, rainfall production and streamflow response in the study area. The new Quantitative Flood Forecasting (QFF) model was applied to predict streamflow peaks with lead-times of 18 and 24 hours over a five year period in 4 watersheds on the leeward side of the Appalachian mountains in the mid-Atlantic region. Threat scores consistently above 0.6 and close to 0.8 ~ 0.9 were obtained for 18 hour lead-time forecasts, and skill scores of at least 40 % and up to 60 % were attained for the 24 hour lead-time forecasts. This work demonstrates that multisensor data cast into an expert information system such as neural networks, if built upon scientific understanding of regional hydrometeorology, can lead to significant gains in the forecast skill of extreme rainfall and associated floods. In particular, this study validates our hypothesis that accurate and extended flood forecast lead-times can be attained by taking into consideration the synoptic evolution of atmospheric conditions extracted from the analysis of large-area remotely sensed imagery. While physically-based numerical weather prediction and river routing models cannot accurately depict complex natural non-linear processes, and thus have difficulty in simulating extreme events such as heavy rainfall and floods, data-driven approaches should be viewed as a strong alternative in operational hydrology. This is especially more pertinent at a time when the diversity of sensors in satellites and ground-based operational weather monitoring systems provide large volumes of data on a real-time basis.

1. INTRODUCTION

Floods are the most frequent natural hazard in the United States: between 1989 and 1999, floods took 988 lives and caused $4.5 billion worth of damage (US Army Corps of Engineers, 1999). Despite many advances in weather forecasting over the last decades, the need for accurate flood forecasting remains as one of the most elusive challenges in operational hydrology.

The methodology adopted to develop a QFF (Quantitative Flood Forecasting) model consists of using neural networks as a data transforming tool combining information from the state of the atmosphere and its recent evolution along with standard hydrometeorological data to issue streamflow forecasts. The structure of the model is dictated by our understanding of the regional hydrometeorology, flood hydrology and by an empirically derived classification that establishes relationships among data from different types of sensors: streamflow and rain gauges, radiosondes, and satellite imagery.

Neural networks have been applied to a wide variety of hydrologic problems such as precipitation forecasting (Kuligowski and Barros, 1998); streamflow prediction (Imrie et al., 2000); and prediction of water quality parameters (Maier and Dandy, 1996) among others. Previous work has demonstrated that neural networks are appropriate to capture the complex nonlinear rainfall-runoff relationships (Campolo et al., 1999). Most previous neural network applications of the rainfall and runoff processes were restricted to short lead-time for accurate forecasts: 1-5 hours (Campolo et al., 1999), 30-75 minutes (Michaud and Sorooshian, 1994). Typically, these studies are based on conceptual rainfall-runoff models and require that raingauges be distributed within and, or near the forecast watersheds. Also, the forecasts are issued after the arrival of rainfall events. Because the rainfall-runoff response times are in the range of a few hours, this constitutes a natural upper bound

on forecast lead-times. Here, our goal is to focus on operational Quantitative Flood Forecasting (QFF) for basins where raingauges are not necessarily available, and to extend the forecast lead-times up to 24 hours in advance, which should provide disaster management agencies with enough time to implement flood control and mitigation measures. The driving hypothesis is that such long lead-times can be attained if the synoptic evolution of atmospheric conditions is taken into consideration. This includes the classification of weather systems as they begin to arrive at the region of interest, and the detection and monitoring of convective weather systems which may or may not be embedded in large-scale storms.

Along the Allegheny Front, in the mid-Atlantic region of the U.S. (Fig. 1), the hydroclimatology of floods is characterized by the recurrence of floods in small to medium watersheds. Such watersheds have a short response time for flooding, and are typically located in regions of complex orography, with narrow valleys and relatively strong relief. Often these watersheds are instrumented with streamflow gauges, but not with raingauges. At these locations, orographic effects on storm duration and intensity lead to the occurrence of heavy rainfall. These watersheds are connected through a dense network of 1st and 2nd order streams, which quickly deliver runoff from headwater catchments to the river valley downstream. When large storms impinge upon this region, the combined contribution of streamflow from these small basins to the main stem of the Susquehanna River leads to extreme floods (Barros and Kuligowski, 1998). Thus, the benefit of improving flood forecasting for such small basins is key to improve flood forecasting in the entire Susquehanna River basin.

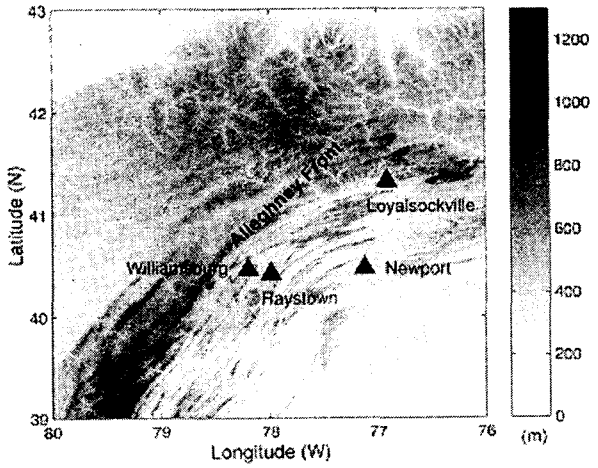

Fig. 1. The digital elevation map of Pennsylvania

In this region, the character of the meteorological scenarios leading to severe flooding events differs between the warm (May through September) and cold (October through April) seasons. In the cold season, floods result from intense and/or lengthy rainfall on dense snowpacks or frozen ground. Here we focus on the wintertime storms that are generally associated with Pacific, Gulf and subtropical Atlantic moisture-rich airmasses. Next , a description of the data used is provided in Section 2, which is followed by a description of the QFF model in Section 3. The application of the model is illustrated for four watersheds in the mid-Atlantic region in Section using both 18 and 24 hours forecast lead-times in Section 4. Final remarks and overall assessment of the approach are presented in Section 5.

2. DESCRIPTION OF DATA

2.1. Satellite Data and Characterization of Convective Weather Systems

The satellite data used to detect and monitor the presence of convective weather systems were obtained from the ISCCP-B3 data set (International Satellite Cloud Climatology Project). The ISCCP-B3 data set provides cloud imagery with temporal resolution of 3 hours and spatial resolution of 30 kms. CCATS (Convection Classification and Automated Tracking System), an algorithm developed by Evans and Shemo (1996) to analyze infrared satellite data such as the ISCCP-B3, was used to detect, classify, and track the evolution of four different types of convective weather systems: tropical cyclones (CYC); mesoscale convective complexes (MCC); convective cloud clusters (CCC); and disorganized short-lived convection (DSL). The classification criteria and the basic characteristics of each convective class are presented in Table 1. For this work, only five years of

data between 1989 and 1993 were available. Note that, because the spatial resolution of the data is 30 kms and summertime thunderstorms in the mid-Atlantic region frequently occur at smaller spatial scales, the applicability of CCATS is limited to mesoscale convective activity during winter and spring. MCCs and CCCs are used in the QFF model as index variables that manifest the character of regional weather.

As the MCC evolves spatially over time, so does the number and locations where rainfall is observed. It should therefore be expected that by forecasting the trajectory of these systems, one should also be able to forecast the space-time evolution of rainfall across the landscape. To be used as input to the QFF model, the convective complexes and clusters were further classified as a function of the location of origin (i.e., where they are first detected) and direction of movement (i.e. direction of the trajectory). For this purpose, the region was subdivided in eight areas, and a spatial climatology of CCCs and MCCs was derived. The quadrants are classified clockwise from North as follows: 1- North; 2- Northeast; 3- East; 4- Southeast; 5- South; 6- Southwest; 7- West; 8- Northwest. Each class is defined for a range of 45° around the labeled direction [-22.5°, +22.5°]. Overall, convective systems move in the E-NE directions, and while MCCs originate mostly in W-SW-S-SE quadrants of the domain, CCCs originate mainly on the S-SE quadrants. This is consistent with the climatology of heavy rainstorms in the region, which are normally associated with southwesterly and southerly weather systems.

Table 1. Definitions and basic characteristics of convective weather systems from satellite cloud imagery (Evans and Shemo, 1996)

Tropical Cyclones (CYC)	
Published storm tracks are used to validate storm tracks analyzed by CCATS.	
A tracking algorithm is used to follow the trajectory of tropical cyclones.	
Systems are matched with MCC or CCC tracks as defined below.	
Mesoscale Convective Complexes (MCC)	
Size	<-54/C region has area >50,000 km^2
Duration	>6 hours (2 frames in the case of ISCCP-B3)
Shape	Eccentricity (minor axis/major axis) > 0.7
Convective Cloud Clusters (CCC)	
Size	<-54/C region has area >50,000 km^2
Duration	6 hours (2 frames in the case of ISCCP-B3)
Shape	No shape criterion
Disorganized, Short-Lived Convection (DSL)	
Size	Temperature <-54C for at least one pixel (i.e. Minimum size determined only by satellite resolution)
Duration	3 hours or less (1 frame in the case of ISCCP-B3)
Shape	No shape criterion

2.2. Radiosonde Data

Data from six radiosonde stations were used in this study. Only directional wind data at 900 hPa, 850 hPa, 800 hPa ,750 hPa, 700 hPa, 650 hPa and 600 hPa pressure levels were used from each radiosonde station. Previous studies of the regional hydroclimatology of rain-producing weather systems in the Central Appalachian Mountains of the United States showed that northerly air masses generally do not cause rainfall in the region, and W-SW-S are prevailing wind directions for rain-producing weather systems (Barros and Kuligowski, 1998). In this study, the characteristics of wind direction for rain-producing weather systems are similar to that of previous research, and we used wind direction data to classify the weather conditions when convective activity was not detected by CCATS.

2.3. Raingauge data

Hourly rainfall from 160 raingauges within the region (45N/85W ~ 33N/70W) were used in this study: 40 in New York- NY; 25 in Ohio-OH; 32 in Pennsylvania-PA; 3 in Maryland-MA; 9 in New Jersey-NJ; 3 in Kentucky-KT; 13 in West Virginia-WV; 16 in Virginia-VA; 3 in Tennessee-TN; 16 in North Carolina-NC. Missing data at these gauges were relatively small: in PA, WV, MD, NJ and VA, the rainfall data exceeded 90% reliability; in NY, OH, KT, TN and NC, the rainfall data exceeded 95% reliability.

2.4. Streamflow gauge data

Because hourly streamflow data are not available for West Virginia, 4 watersheds were selected in Pennsylvania with areal extent ranging from 750 km^2 to 8,700 km^2 : Williamsburg, Raystown, Loyalsockville and Newport. The locations of the streamflow gauges corresponding to these watersheds are shown in Fig.1. The four watersheds selected have often experienced severe flooding in the past, and particularly in connection with major floods in the Susquehanna River basin (Barros and Kuligowski, 1998).

3. DESCRIPTION OF THE QUANTITATIVE FLOOD FORECASTING MODEL

The overall approach to develop the QFF model consisted in developing a multisensor data-driven model using an expert system of neural networks, the configuration of which is determined by regional hydroclimatology, operational data availability, and forecast criteria. Hourly streamflow and rainfall data are used to describe rainfall-runoff response, while radiosonde and satellite data are used to describe the evolving structure of regional weather. This approach evolved from an existing Quantitative Precipitation Forecasting (QPF) model, which was used to forecast point rainfall 6 to 12 hours in advance at more than one location using only raingauge data and output from Numerical Weather Prediction (NWP) models (Kuligowski and Barros, 1998). The existing QPF model was greatly modified to handle multisensor data at large spatial scales, and to issue streamflow forecasts with long lead-times. Specifically, the foremost forecast criterion is to capture the timing and magnitude of peak flood discharge at least 18 hours in advance.

The QFF model consists of three different modules. In the first module, the raingauges are surveyed to look for rainfall occurrences. If no rainfall is detected in the study area, a no-rain forecast is used. Next, the classification and decision module is used to describe and classify current weather conditions using radiosonde and satellite data. A second rain/no rain forecast is issued based on the likelihood that rain may, or may not occur at the forecast locations within the prescribed lead-time (i.e. the next 18-24 hours). If a positive rain forecast is issued by the second module, then the configuration of the neural network model will be selected according to the weather conditions (e.g. weather class) and as a function of input data available. Finally, the forecast module consists of a system of neural network models with at least four different configurations for each weather class. Hourly rainfall at four locations (i.e. predictor raingauges) and streamflow at the predicted gauge are respectively the inputs and outputs to the selected neural network model. The neural network output is an hourly streamflow forecast at the desired location at the desired time (desired time = current time + forecast lead-time). Detailed descriptions of the classification and forecast modules are presented next.

3.1 Weather Classifier

Appropriate selection of the neural network model configurations depends on the effectiveness of the weather classification module in relating streamflow at a specific location, rainfall at four raingauges, and regional atmospheric conditions. Indeed, a key element of the QFF model is the selection of the four predictor raingauges among the 160 raingauges available, which will be used as input to the neural network. Bardossy et al. (1995) developed a semi-automated classification scheme of daily atmospheric circulation patterns using a fuzzy-rule based approach and the expert knowledge of the meteorologist. This combines advantages of automated and manual classification methods. In this study, we used a more physical classification method using expert knowledge of convective weather system with conditional correlation analysis. Analysis of model performance according to the different weather classification methods remains a challenging topic.

The optimal combination of predictor raingauges for each weather class was selected based on statistical analysis between the 4 streamflow gauges and the 160 raingauges. Correlation analysis between streamflow and rainfall was conducted for each forecast location as a function of the weather class type (e.g. MCC or CCC), origin and moving direction of the weather system, and also as a function of the distance between its current location of the weather system and its location at the time for which the forecast is issued. Two zones of influence were considered: zone1 and zone 2, respectively for distances less than and greater than 300 km, the characteristic spatial scale of synoptic weather systems in the mid-Atlantic region. When more than one type of weather system was identified, the priority was given to MCCs over CCCs, and when several convective systems of the same type were identified, the priority was given to the weather system nearest to the streamflow gauge for which location the forecast is desired (i.e. the predicted location). For each weather class, the four raingauges that exhibit the highest correlation with the streamflow gage were selected as predictor gauges. For each weather class, a suite of neural network models was subsequently trained using the data from the corresponding four predictor raingauges as input.

When no convective systems are detected in the satellite imagery, the weather classification is made according to the radiosonde wind data. The predictor raingauges are selected in this case as a function of the wind direction at the radiosonde location, and at the pressure level for which the highest correlation between streamflow and rainfall occurs when southwesterly storm systems approach the area of interest. This criterion is based on the regional hydroclimatology of floods that relates southwesterly rainstorms with heavy precipitation and extended flooding as mentioned earlier in the manuscript. In fact, about 70% of all weather systems approach the lee side of the Appalachian mountains from the W-SW-S, which is consistent with the predominant trajectories of convective systems.

3.2. Neural Networks

Artificial neural networks are data-processing systems that can learn the relationships between a pair of one- or multi- dimensional data sets by tuning a set of model parameters. These parameters (weights) form a mapping from a set of given values (inputs) to an associated set of values (outputs). The process of tuning the weights to the correct value (i.e. training) is carried out by passing a large number of input-output pairs through the model and adjusting the weights to minimize the error between the observed and predicted data. The practical advantages and limitations of neural networks in forecast applications have been discussed by Kuligowski and Barros (1998) among others. In principle, the self-learning nature of a neural network allows it to forecast without extensive prior knowledge of all the processes involved. However, because data analysis techniques are unable to evaluate the generality of the relationships that they find, the data sets used for training must be representative of the physically-based dynamical range of the forecasts. That is why the application of neural networks in environmental problems cannot be successful without a good understanding of the physics involved, and without a hypothesis as to how different processes (and their state variables) interact with each other.

In this study, the neural networks are composed of three layers including input layer, hidden middle layer, and output layer. Each node of the hidden layer receives a signal from every node in the input layer. Besides the data at the four predictor raingauges, the current streamflow is also used as input to the neural network model. The number of nodes in the hidden layer is an important parameter with respect to the computational efficiency of the neural network model. Fletcher and Goss (1993) proposed a number ranging from (2n+1) to ($2n^{0.5}$+m), where n is the number of input nodes and m is the number of output nodes. Although this formula provides an useful guideline, the best results are obtained by trial-and-error experiments (Kuligowski and Barros 1998). In the case of our applications, best results were obtained using only three hidden layer nodes. The effective incoming signal to node j is the weighted sum of all input signals:

$$h_j = \sum_{i=1}^{m} w_{ji} r_i \qquad (j = 1,.....,n) \tag{1}$$

where m is the total number of neurons in the input layer, n is the total number of neurons in the hidden layer, w is the weight assigned to the path from i to j, r_i is input from unit i and h_j is value at unit j of hidden layer. Subsequently, the combined signal is modified by the so-called transfer function to produce the output signal:

$$o_k = \sum_{j=1}^{n} w_{kj} f(h_j) = \sum_{j=1}^{n} w_{kj} f\left(\sum_{i=1}^{m} w_{ji} r_i \right) \qquad (k = 1,.....,l) \tag{2}$$

where f denotes the selected transfer function, w is the weight assigned to the path from j to k, o_k is network output and l denotes total number of nodes in the output layer.

A nonlinear transfer function (the sigmoidal function) allows the neural networks to consider nonlinear relationships between input and output data:

$$f(h) = \frac{2}{1 + \alpha e^{-h}} - 1 \tag{3}$$

where h is input to the node, $f(h)$ is the node output, $\forall$ is the gain which is introduced to consider nonlinear behavior of input data.

The training process consists in determining a new set of weights that minimizes the mean squared error E of the output:

$$E = \sum_{k=1}^{l} (t_k - o_k)^2 \tag{4}$$

where t_k is the desired output at the output node k..

Because the transfer function is nonlinear, the error E will be a nonlinear function of the weights w. The steepest descent method was the nonlinear minimization technique adopted. Accordingly, the weights are adjusted as follows:

$$\Delta w_{ji} = -\eta' \frac{\partial E}{\partial w_{ji}} = -(1-\beta)\eta' \frac{\partial E}{\partial w_{ji}} + \beta(\Delta w_{ji})_{old} = \eta \frac{\partial E}{\partial w_{ji}} + \beta(\Delta w_{ji})_{old} \quad (5)$$

where η is learning rate which tells the network how quickly the weights must be changed and β is the fraction of average change in the weights. The momentum term $\beta(\Delta w)_{old}$ is added to the weight adjustment to avoid local minima. Both η and β are typically between zero and one, and are estimated by trial and error method. Values of 0.001 for the learning rate η, 0.01 for the fraction of average change in weights β, and 2.0 for the gain parameter $\forall$ gave satisfactory results for the applications reported here.

4. RESULTS AND DISCUSSION

Table 2 provides a description of the four neural network model configurations used to issue four different types of forecasts in this study. These configurations were designed to reflect limitations associated with data availability and the type of forecast as well. The C4 configuration aims at forecasting the highest flood peaks, and can only be used if convective systems have been detected in the study region. The R4 configuration serves the same purpose of C4, but is used only when no convective systems have been detected. In the R3 configuration, only radiosonde data are used and forecasts are issued at all times. Thus, while the purpose of the C4 and R4 configurations is to capture the extremes, the purpose of the R3 configuration is to provide forecast coverage for all weather conditions. The combined forecast is a product obtained by selecting the highest forecast among C4, R4 and R3 outputs at all times.

Table 2. Summary of the different neural network configurations used in the QFF model

Model	Input Data Type
C4	· Convective weather systems are present, and all predictor raingauges are wet.
C3	· Convective weather systems are present, and more than 75% of predictor raingauges are wet.
R4	· Convective weather systems have not been detected, and all predictor raingauges are wet.
R3	· Convective weather systems have not been detected, and more than 75% of predictor raingauges are wet.
Combined	· Various combinations of C4, C3, R4 and R3 based on data availability.

Given that only five years of ISCCP-B3 data were available, model performance was evaluated using cross-validation to maximize the amount of data available for training: that is, the model was trained for each possible combination of four five-month periods (December-January-February-March-April), and the 5th was used to evaluate model performance. In this manner, performance statistics can be generated for the entire 5-year period.

The combined forecast product is presented in Fig. 2(a), whereas Figs. 2(b)-(c) are zooms of the Fig.2(a) at different times to illustrate the overall quality of the QFF model performance. Overall, the figures show that peak streamflow values are captured well, and timing errors are small. Five quantitative measures of forecast skill were calculated to evaluate the model performance: 1) the skill score defined as the percentage reduction in the mean-squared error with respect to persistence forecasting method; 2) the correlation coefficient, which describes the strength of the linear relationship between forecasts and observations; 3) the bias defined as the degree of correspondence between the mean forecast and the mean observation; 4) the root mean squared error defined as the sum of square of the differences of the forecasts and observations; and 5) the threat score, a categorical verification measure equal to the total number of correct event forecasts (hits) divided by the total number of flood forecasts plus the number of misses as used in Kuligowski and Barros (1998).

A summary of the skill scores is provided in Tables 3 for 18 hours forecast lead-times. The skill scores are very high in comparison with the skill of Quantitative Precipitation Forecasts used to drive standard operational flood forecasting models, especially in the case of 18-hour lead-times. Again, especially remarkable are the skill scores obtained with the C4 configuration. To examine the results in more detail, Figs. 3(a)-(d) illustrate the variation in threat scores for the different model configurations and different thresholds, that is the 25th, 20th, 15th, 10th, and 5th streamflow percentiles. As expected, the 18-hour forecasts are better overall than the

24-hour forecasts, but the real message implied by these results is that value-added forecasting skill by using the inherently synoptic and dynamical satellite data should not, and must not be ignored in operational flood forecasting. In addition, the performance of the QFF model was very similar for all four watersheds, showing that forecast skill is not sensitive to the spatial scale of the watershed upstream of the forecast location.

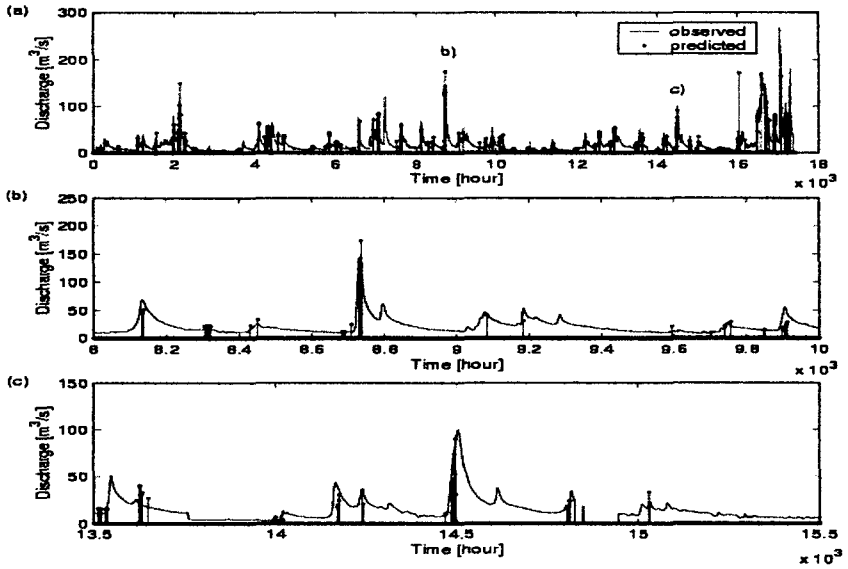

Fig. 2. (a) Time series of observed streamflow and the 18-hr lead-time combined forecasts at Williamsburg from December to April between 1989 and 1993 periods; (b) and (c) are enhanced zooms of short duration periods to illustrate model performance.

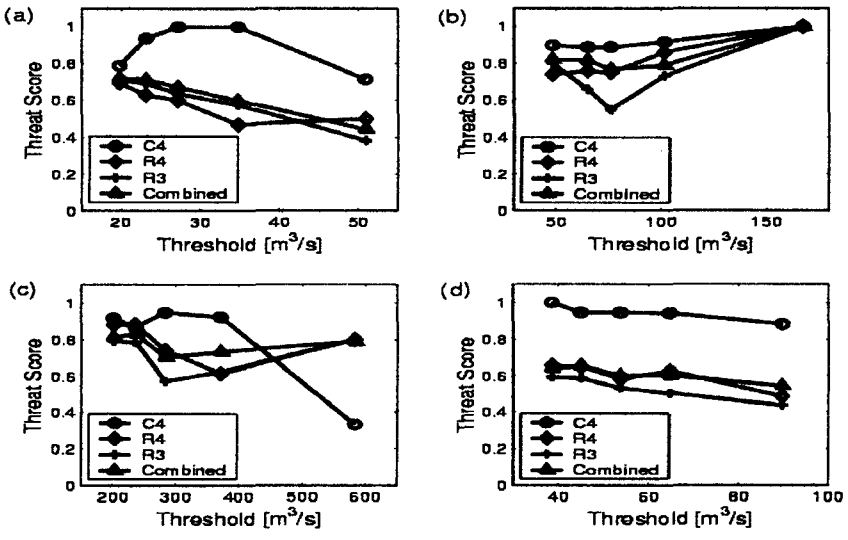

Fig. 3. Variation of threat scores for the 18 hour lead-time forecasts using the different neural network model configurations: (a) Williamsburg; (b) Raystown; (c) Newport; (d) Loyalsockville. Thresholds are 25, 20, 15, 10 and 5 percentiles of streamflow for each location.

Table 3. Statistical performance measures of the QFF model for forecast lead-times of 18 hours.

Name	Model	Tr#	RMSE	SS	CC	Bias	Threat Scores				
			(m^3/s)			(m^3/s)	25 %	20 %	15 %	10 %	5 %
Williamsburg	C4	10	11	0.96	0.97	3	0.79	0.94	1.00	1.00	0.71
	R4	10	33	0.62	0.72	-1	0.69	0.63	0.60	0.47	0.50
	R3	500	23	0.32	0.72	5	0.71	0.69	0.64	0.58	0.38
	Combined	-	23	0.54	0.75	3	0.72	0.71	0.67	0.60	0.44
Raystown	C4	10	20	0.93	0.96	-3	0.90	0.89	0.89	0.92	1.00
	R4	10	20	0.78	0.88	1	0.74	0.76	0.75	0.86	1.00
	R3	100	32	0.54	0.91	-2	0.80	0.66	0.55	0.73	1.00
	Combined	-	28	0.79	0.93	-5	0.82	0.82	0.77	0.79	1.00
Newport	C4	10	78	0.89	0.93	21	0.92	0.87	0.95	0.92	0.33
	R4	10	139	0.51	0.89	33	0.88	0.88	0.74	0.61	0.80
	R3	50	136	0.22	0.91	13	0.79	0.79	0.57	0.62	0.80
	Combined	-	115	0.56	0.93	-6	0.81	0.83	0.70	0.73	0.79
Loyalsockville	C4	10	94	0.81	0.76	22	1.00	0.94	0.94	0.94	0.88
	R4	10	138	0.30	0.59	46	0.66	0.65	0.58	0.63	0.49
	R3	100	95	0.18	0.52	18	0.68	0.69	0.63	0.59	0.55
	Combined	-	88	0.39	0.65	11	0.69	0.69	0.64	0.61	0.61

5. CONCLUSIONS

In this study, we developed an operational forecasting model for ungauged watersheds in the mid-Atlantic region using a data-driven approach which makes use of satellite, radiosonde, streamflow and rainfall data. This study validates our hypothesis that accurate and extended flood forecast lead-times can be attained if the synoptic evolution of atmospheric conditions is taken into consideration. Threat scores consistently above 0.6 and close to 0.8 ~ 0.9 were obtained for 18 hour lead-time forecasts, and skill scores of at least 20 % and up to 60 % were attained for the 24 hour lead-time forecasts.

One contribution of this work is to demonstrate that multisensor data cast into an expert information system such as neural networks, if built upon scientific understanding of regional hydrometeorology, can lead to significant gains in the forecast skill of extreme rainfall and associated floods. While physically-based numerical weather prediction and river routing models cannot accurately depict complex natural non-linear processes, and thus have difficulty in simulating extreme events such as heavy rainfall and floods, data-driven approaches should be viewed as a strong alternative in operational hydrology. This is especially more pertinent at a time when the diversity of sensors in satellites and ground-based operational weather monitoring systems provide large volumes of data on a real-time basis. Further details can be found in Kim and Barros (2001).

REFERENCES

Bardossy, A., Duckstein, L., and Bogardi, I. (1995) "Fuzzy rule-based classification of atmospheric circulation patterns" *Int. J of Climatol.*, Vol. 1, No. 15, pp. 1087-1097

Barros, A.P., and Kuligowski, R.J. (1998) "Orographic effects during a severe wintertime rainstorm in the Appalachian Mountains" *Mon. Weather Rev.* Vol. 126, pp. 2468-2772.

Campolo M., Andreussi, P., and Soldati, A. (1999) "River flood forecasting with a neural network model" *Water Resour. Res.* Vol. 35, No. 4, pp. 1191-1197.

Evans, J.L., and Shemo, R.E. (1996) "Automated identification and climatologies of various classes of convection in the Atlantic Ocean" *J. Appl. Meteorol.* Vol. 35, pp. 638-652.

Fletcher, D.S., and Goss E. (1993) "Forecasting with neural networks: An application using bankruptcy data" *Inf. Manage.* Vol. 24, pp. 159-167.

Imrie, C.E., Durucan, S., and Korre, A. (2000) "River flow prediction using artificial neural networks: generation beyond the calibration range" *J. Hydrol.* Vol. 233, pp. 138-153.

Kim, G., and Barros, A.P. (2001) "Quantitative flood forecasting using multisensor data and neural networks" *J. Hydrol.* Vol. 246, pp. 45-62.

Kuligowski, R.J., and Barros, A.P. (1998) "Localized precipitation forecasts from a numerical weather prediction model using artificial neural networks" *Weather and Forecast.* Vol. 13, No. 4, pp. 1194-1204.

Michaud, J., and Sorooshian S. (1994) "Comparison of simple versus complex distributed runoff model on a midsized semiarid watershed" *Water Resour. Res.* Vol. 30, No. 3, pp. 593-605.